PET Hydroxyephedrine Imaging of Neuroblastoma

Barry L. Shulkin, Donald M. Wieland, Marie E. Baro, David R. Ungar, Deanna S. Mitchell, Mukund G. Dole, Jawhar B. Rawwas, Valerie P. Castle, James C. Sisson and Raymond J. Hutchinson

Department of Internal Medicine and Division of Nuclear Medicine, Department of Pediatrics and Communicable Diseases, University of Michigan Medical Center, Ann Arbor, Michigan

The goals of this investigation were to characterize the uptake of ^{11}C-hydroxyephedrine (HED) in neuroblastoma and to determine the feasibility and potential advantages of utilizing this compound as a tumor imaging agent. **Methods:** Seven patients with known or subsequently proven neuroblastoma were studied. Each patient underwent PET scanning with ^{11}C-HED. Six of seven patients underwent scintigraphy with [^{123}I]meta-iodobenzylguanidine (MIBG), and two patients were also studied with [^{18}F]FDG PET. For six patients, CT or MR images were available for comparison. **Results:** Neuroblastomas were located by PET scanning with ^{11}C-HED in all seven patients. The uptake of HED into neuroblastomas was rapid; tumors were evident on images within 5 min postintravenous injection. Those lesions in the field of view of the PET camera were also identified on [^{123}I]MIBG scintigraphic images. In two patients, tumor deposits in the abdomen were better visualized with MIBG scintigraphy due to relatively less hepatic accumulation of MIBG than HED. **Conclusion:** PET scanning with HED for neuroblastoma results in high quality functional images of the tumors that can be obtained within minutes following injection.

Key Words: PET; neuroblastoma; carbon-11-HED; iodine-123-MIBG; fluorine-18-FDG

J Nucl Med 1996; 37:16–21

Neuroblastoma is the most common solid extracranial malignancy of childhood (*1,2*). Due to their neuroendocrine origin from cells which form components of the sympathetic nervous system, these tumors retain the capacity to accumulate catecholamines and related substances. The detection of neuroblastoma was advanced by the introduction of meta-iodobenzylguanidine (MIBG), the first radiotracer used to image elements of the sympathetic nervous system and related tumors in humans (*3–5*). Scintigraphy with MIBG enables noninvasive screening of the entire body for deposits of pheochromocytoma or neuroblastoma. The method is both sensitive (>90%) and specific (>95%) for neuroblastomas, and is especially helpful in identifying these tumors outside the adrenal gland, metastatic disease and those that are recurrent (*6,7*). The imaging characteristics of [^{131}I]MIBG, however, are not ideal since:

1. The gamma photons are highly energetic, and only 20% are detected by modern cameras.
2. A substantial amount of radiation is imparted as beta particles, which are not detected by gamma cameras.
3. The physical half-life (8.1 days) is relatively long.

Each of these features restricts the activity that can be administered. Since the highly lipophilic iodophenyl portion of MIBG may result in nonspecific binding to cell membranes early after injection, optimal tumor-to-nontumor ratios are not achieved until a day or more after injection. MIBG labeled with ^{123}I overcomes some of the disadvantages of [^{131}I]MIBG and produces high quality images, but there are several shortcomings (*7*), including limited availability, expense, delay between injection and imaging, the frequent need for two imaging sessions and, on occasion, false-negative results.

Carbon-11-hydroxyephedrine (HED) is a new radiotracer developed to image the sympathetic nervous system (*8*). The aromatic portion of HED is less lipophilic than that of MIBG and while HED bears closer structural similarity to norepinephrine, it is not metabolized as is norepinephrine. Biodistribution studies in experimental animals and humans have shown selective uptake in organs with rich sympathetic innervation, including the heart and adrenal medulla. When HED is labeled with ^{11}C, its distribution can be portrayed in vivo using PET. This agent has been used to map the sympathetic innervation of the heart, and we have previously shown that HED is highly concentrated in deposits of pheochromocytoma (*9–11*). PET offers improved imaging capability over conventional single-photon techniques:

1. The use of agents labeled with short-lived radionuclides enables administration of larger tracer doses and, consequently, images of higher count density and superior quality.
2. Multiple short-lived tracers can be administered within a single session to assess various biological aspects of the tumor or the effects of an intervention.
3. The intrinsically tomographic nature of the technique allows for the more precise depiction of spatial relationships of tumors and nearby organs than does planar imaging, although the quality of SPECT images with multiheaded gamma cameras rivals that of PET images.
4. Quantification of tumor uptake may be performed.

We hypothesized that neuroblastomas would rapidly concentrate HED and that by using PET to detect focal accumulations of HED, both the anatomic site and the functional nature of these adrenergic tumors would be portrayed in high quality images within minutes after injection. The goals of this investigation were to evaluate the feasibility and potential utility of PET scanning with HED for localizing neuroblastomas (*12,13*).

METHODS

The study was approved by the Institutional Review Board for Approval of Research involving Human Subjects and the Subcommittee for Human Use of Radioisotopes of the University of Michigan. Written informed consent was obtained from Patient 1 and a parent of each of the other patients.

Patients

Seven subjects (4 male, 3 female), aged 6 mo to 27 yr, with known or subsequently confirmed neuroblastoma were studied (Table 1). Patients 1–5 and 7 had previously undergone chemotherapy and/or resection of neuroblastoma and had recurrent or persistent disease. Patient 6 was studied upon initial presentation. None of the subjects was receiving treatments known to interfere with the transport of catecholamines into the sympathetic neuronal terminals (*14,15*).

Received Sept. 6, 1994; revision accepted May 15, 1995.

For correspondence or reprints contact: Barry L. Shulkin, MD, Pediatric Nuclear Medicine, MCHC F3313, University of Michigan Medical Center, 200 E. Medical Center Dr., Ann Arbor, MI 48109-0229.

TABLE 1
Patient Data

Patient no.	Sex	Age (yr)	HED scan	Tumor HED uptake	Tumor MIBG uptake	Reference organ
1	F	27	Uptake in disease recurrence at diaphragm (Fig. 1)	+3	+3	Liver
2	M	3	Uptake of HED in disease recurrence in skull	+3	+3	Brain
3	M	0.5	Uptake into pelvic mass (Fig. 2)	+3	+3	Soft tissue
4	M	9	Uptake into persistent abdominal disease (Fig. 4)	+3	+3	Liver
5	M	3	Uptake into recurrent disease in vertebral body	+1	+3	Liver
6	F	2	Uptake into mostly necrotic large abdominal mass, extensive bone marrow uptake	+1	*	Liver
7	F	7	Uptake in thigh muscle and iliac wing	+3	+2†	Muscle

*MIBG study not performed.
†See text for times of MIBG and HED scans. Scans were reviewed by two of the authors. There were no disagreements between their independent conclusions.

Imaging studies consisted of PET scanning with ^{11}C-HED and [^{123}I]MIBG scintigraphy. In two patients, [^{18}F]FDG PET scanning was performed within 5 wk of the HED and MIBG studies. In six patients, anatomic imaging with CT or MRI was available for comparison.

HED-PET

Radiochemistry. The synthesis of ^{11}C-HED has been described in detail elsewhere (*8*). Briefly, ^{11}C-HED was produced by direct N-methylation of metaraminol with ^{11}C-methyl iodide in DMF/DMSO and purified by reverse-phase HPLC in an isotonic aqueous buffered system. The specific activity was >1000 Ci/mmole at the end of synthesis, and radiochemical and chemical purities were 95%–98%.

Data Acquisition and Reconstruction. Patients were positioned in a whole-body PET scanner with the principal tumor centered in the middle of the field of view. Following a 10–20-min transmission scan for attenuation correction using a retractable ^{68}Ge source, the patients received an intravenous injection of 5 mCi ^{11}C-HED (Patient 1, an adult subject, received 20 mCi). Imaging of the tumors was begun immediately after tracer administration and continued for 30 min. This was followed by a limited screen for metastatic disease covering 40–60 cm in the z-axis in most patients. In Patient 1, an additional 10-min view of the principal tumor was obtained 60 min postinjection.

Data were reconstructed into transverse cross-sectional images using filtered backprojection and a Hanning filter with a cutoff frequency of 0.35 per pixel.

FDG-PET

In Patients 2 and 3, PET scanning with [^{18}F]FDG was performed approximately 4 hr after the patient's last feeding. For the study of Patient 2, 133 MBq (3.6 mCi) [^{18}F]FDG were administered intravenously while the patient sat quietly with eyes open in a dimly lit room. Thirty minutes postinjection, images of the head and brain were obtained for 30 min. For the study of Patient 3, a 10-min transmission scan of the abdomen and pelvis for attenuation correction was obtained using a retractable ^{68}Ge source. Emission images were acquired for 50 min following intravenous administration of 93 MBq (2.5 mCi) [^{18}F]FDG. Data were reconstructed as previously described.

MIBG Scintigraphy

Patients 1–5 underwent [^{123}I]MIBG scintigraphy within 3 wk of the PET examination. Patient 7 was studied with MIBG 3 wk prior to and 4 wk following PET scanning. Patient 6 did not undergo MIBG scintigraphy.

Data Acquisition and Reconstruction

After intravenous administration of 370 MBq (10 mCi)/1.7 sq m [^{123}I]MIBG, planar and tomographic images were obtained (*15*).

Planar. Anterior views of the entire body and posterior views of the chest and abdomen were acquired 24 hr postinjection. Anterior views from the head to the knees and posterior views of the chest and abdomen were acquired 48 hr postinjection (Only 1 patient underwent imaging 2 hr postinjection). Each image was obtained for 10 min. A gamma camera with a low-energy collimator interfaced to a computer was used.

SPECT. Tomography was performed 24 hr (and 2 hr in Patient 1) postinjection using a gamma camera with a low-energy collimator (a triple-head gamma camera was used for Patient 4). The camera was rotated through 360° with 64 stops of 20 sec each. Data were reconstructed using filtered backprojection, a Butterworth filter and a cutoff frequency of 0.2–0.5. From the transverse reconstructions, regions of interest (ROIs) were defined over the tumor and adjacent background, analogous to the PET examination.

Image Analysis

Images were reviewed by two nuclear imaging physicians. Tumor uptake of HED was assessed qualitatively and quantitatively.

Qualitative Analysis. From studies previously performed in normal volunteers and in patients with pheochromocytoma, organs that normally accumulate the tracers were identified by visual inspection. Sites of accumulation that did not appear in normal volunteers and did not conform to usual anatomic configurations were considered abnormal. A scale was used to visually assess tumor uptake with reference to a normal appearing organ (usually the liver) in the field of view: 0 = no uptake, +1 = vague uptake less than the normally appearing organ, +2 = uptake equal to a normally appearing organ and +3 = uptake greater than a normally appearing organ (Table 1).

Quantitative Analysis. ROIs were placed over the tumor and identifiable noninvolved organs, including the liver and kidney when within the field of view from images obtained 30 min following injection of HED. Irregular ROIs were constructed about the entire tumor and ranged in sized from 43 to 208 pixels, depending on the size of the tumor. Reference organ ROIs ranged from 30 to 165 pixels. These regions were copied to all time frames and time-activity curves were generated. Activity was also normalized to the injected dose. Tumor-to-nontumor ratios of radioactivity were calculated. ROIs of similar size and shape were drawn for

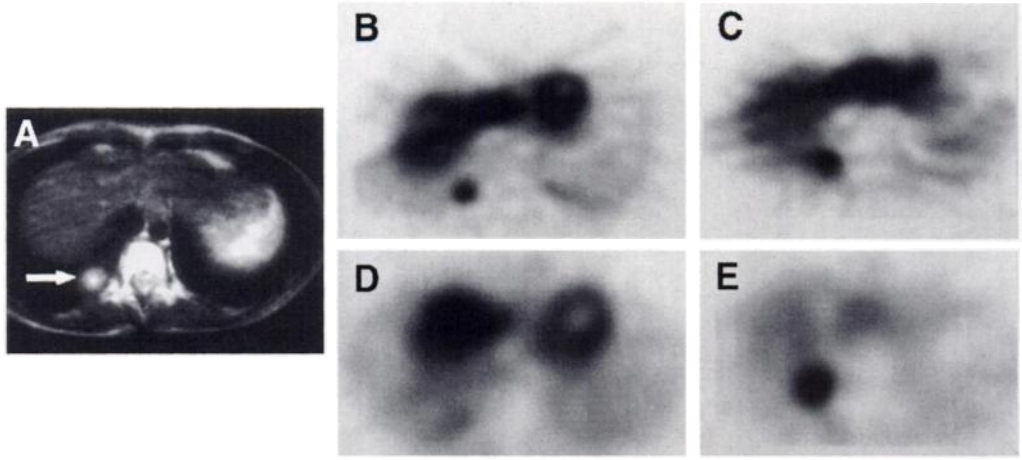

FIGURE 1. Patient 1. (A) T2-weighted transverse MR image of the lower chest-upper abdomen. A mass with high signal intensity is seen in the posterior right lung field. (B) HED-PET scan at same level acquired 10 min postinjection. There is intense uptake within the right posterior lung mass. (C) HED-PET image 60 min postadministration: Good uptake remains within the mass, demonstrating the high retention of HED. (D) MIBG-SPECT scan 2 hr postinjection shows no definite uptake within the mass. (E) MIBG-SPECT examination at 24 hr. By this time, there is clear accumulation of MIBG within the tumor, confirming its adrenergic nature. The tumor was removed surgically and shown to be neuroblastoma.

SPECT images and ratios of tumor-to-reference organ activity were calculated.

RESULTS

PET scanning with ^{11}C-HED detected foci of neuroblastoma in all 7 patients rapidly and clearly. Images from Patient 1 are presented in Figure 1. This 27-yr-old woman had undergone resection of a ganglioneuroblastoma 4 yr earlier. A routine follow-up CT scan showed a 2-cm soft-tissue mass in the posterior right lung. Figure 1 depicts the accumulation of ^{11}C-HED and [^{123}I]MIBG by the mass. Intense uptake of ^{11}C-HED is apparent in the tumor by 10 min and stable retention through 60 min postinjection (Figs. 1B, C). Hepatic and cardiac uptake are also present. The tumor-to-liver ratios at 10 and 60 min were 0.7 and 1.1. At 2 hr following intravenous administration of 10 mCi [^{123}I]MIBG, there was no definite accumulation of MIBG within the tumor (Fig. 1D). By 24 hr, however, there was high uptake of MIBG within the tumor (Fig. 1E). The tumor-to-liver ratio at 24 hr was 3.1. Histologic examination of the tumor confirmed the diagnosis of neuroblastoma. The rapid accumulation and high retention of HED in this patient's neuroblastoma suggested that this technique may be an additional imaging modality for the detection and monitoring of neuroblastoma.

Patient 3 is a 6-mo-old boy with Stage IV neuroblastoma. He was born with massive hepatomegaly causing respiratory compromise. He received radiotherapy to the right upper quadrant for symptomatic relief. At 6 mo of age, he underwent surgical debulking of a right-sided pelvic mass which was confirmed histologically as neuroblastoma. Postoperative CT scanning showed residual tumor, which accumulated MIBG (Fig. 2). The patient underwent PET scanning with HED and FDG (Fig. 2). Although the tumor accumulated both positron-emitting radiotracers, uptake of HED was greater than that of FDG [%ID/gram of tumor was 0.058 (HED) and 0.022 (FDG)]. Patient 2 also underwent PET scanning with FDG. Although this patient's metastatic disease in the skull clearly accumulated both HED and MIBG, there was no abnormal uptake of FDG.

All known lesions within the field of view of the PET camera (i.e., those seen by MIBG scanning) were visualized. The

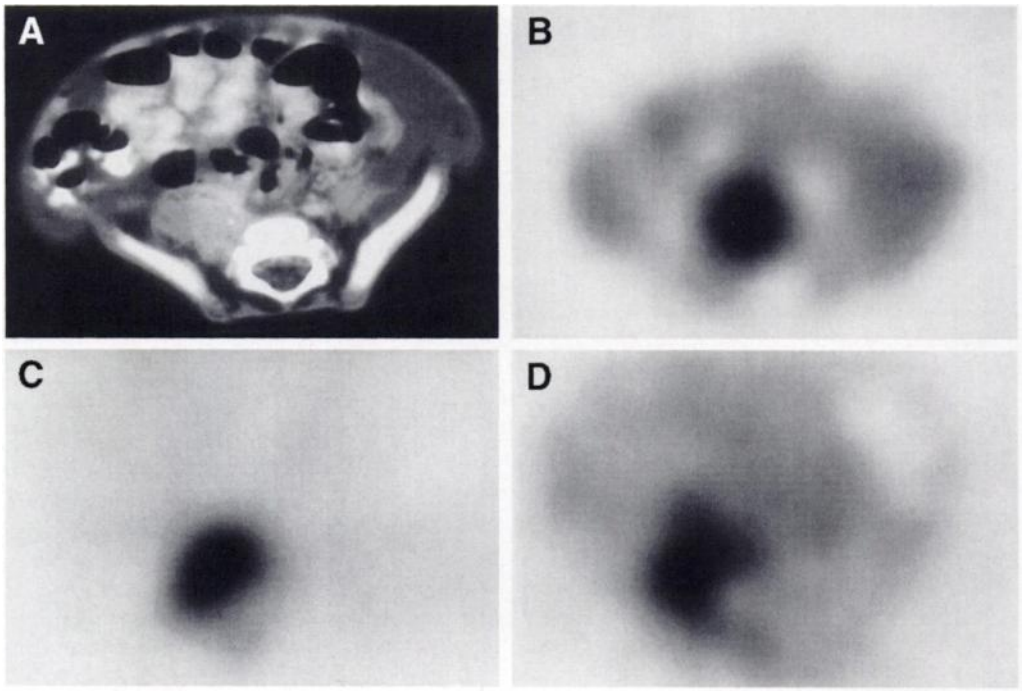

FIGURE 2. Patient 3. (A) CT scan of the pelvis at 6 mo of age following surgical debulking: There is abnormal soft tissue with speckled calcification in the right posterior pelvis. (B) MIBG-SPECT scan at 24 hr shows uptake into the tumor. (C) HED-PET scan 20 min postinjection. There is excellent uptake within the neuroblastoma, and the image appears similar to the MIBG-SPECT image. (D) FDG-PET scan at 50 min postinjection. There is moderate accumulation of FDG within the mass relative to surrounding background. The tumor, however, appears better delineated with HED.

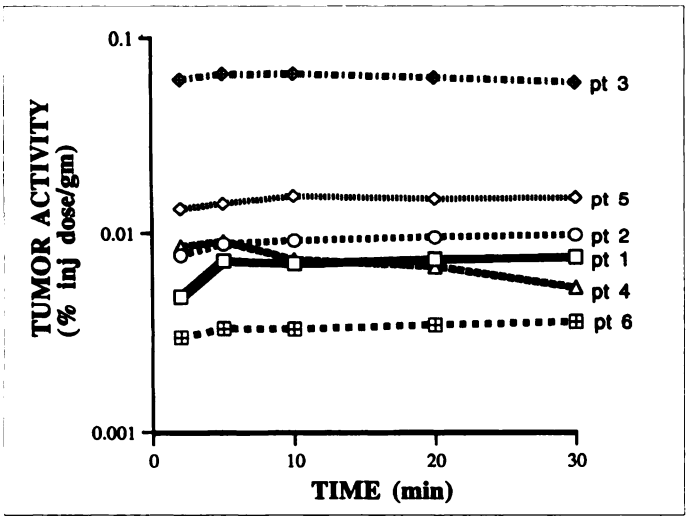

FIGURE 3. Tumor accumulation (Patients 1–6) as a function of time. The x-axis value is minutes postinjection of HED. The majority of uptake of HED occurs within 2 min of injection. Retention of activity was high, with the exception of the tumor of Patient 4, whose activity declined substantially from peak levels.

uptake of HED into deposits of neuroblastoma was rapid. By 2 min, 80% of the mean maximal uptake had occurred. The time-activity graphs for the neuroblastomas of Patients 1–6 are shown in Figure 3. In four patients, HED uptake into the tumors continued through 30 min, the termination point of the dynamic sequence. In Patients 3 and 4, uptake peaked within 10 min following injection. In Patient 4, there was substantial tracer loss from the tumor, with only 58% of maximal activity retained at 30 min.

Hepatic uptake was prominent and liver uptake exceeded tumor uptake in four of the five patients with abdominal disease. Figure 4 displays the tumor-to-liver accumulation over time. The tumor-to-liver ratio increased steadily throughout the course of the dynamic imaging session. This was largely due to progressive decline in liver activity beginning 3 min postinjection in the face of steady tumor activity. There were two patients whose disease appeared better defined with MIBG due to relatively less hepatic accumulation of MIBG than HED. Figure 5 shows the HED and MIBG scans for Patient 4, a 9-yr-old boy with persistent abdominal neuroblastoma following chemotherapy and radiotherapy. There was good uptake of HED within the tumor as well as normal hepatic uptake and renal excretion. In contrast there was very little background MIBG activity in the liver and kidneys at 24 hr. Thus, the tumor was more apparent. Tumor-to-liver ratios were 0.97 for HED at 30 min and 1.9 for MIBG at 24 hours.

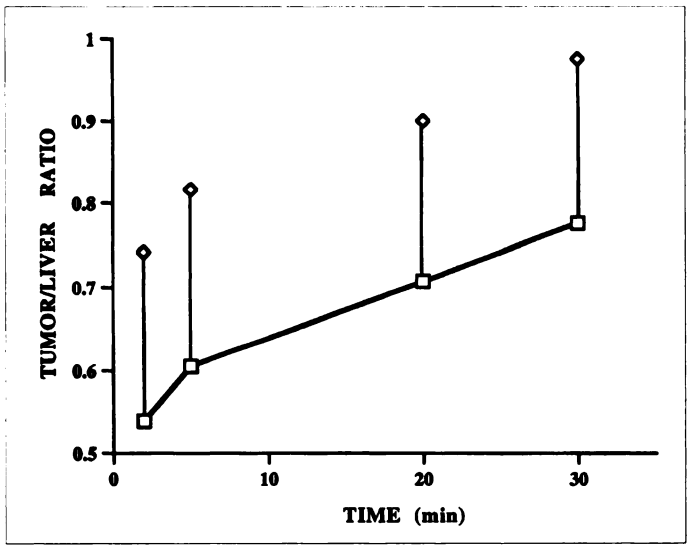

FIGURE 4. Tumor-to-liver ratios (mean + s.d.) for HED-PET as a function of time (Patients 1, 4–6, the livers of Patients 2 and 7 were not included in the attenuation-corrected image field, and the liver of Patient 3 contained neuroblastoma). The progressive rise in tumor-to-liver activity ratios is largely due to clearance from the liver.

Renal uptake and excretion of HED were also high soon after injection. Peak renal activity occurred 3–4 min after injection and rapidly declined to 8%–40% of maximal values at 30 min due to excretion into the urinary tract.

Patient 6 did not undergo MIBG scintigraphy. This patient presented with a large left-sided abdominal tumor. CT imaging identified marked intrarenal extension and central necrosis. The diagnosis of neuroblastoma was established by detecting the tumor in bone marrow. There was HED uptake about the periphery of the tumor but the bulk of the tumor did not concentrate HED. Diffuse skeletal uptake of HED, consistent with bone marrow involvement, was also evident. The patient developed life-threatening renal and pulmonary complications following initiation of chemotherapy. She suffered an early demise and MIBG imaging could not be performed.

There was one patient whose uptake of HED is likely, but not definitely, due to tumor (Patient 7). MIBG scanning 3 wk prior to HED-PET showed widespread skeletal neuroblastoma. The patient suffered progressive thigh pain. There was no history of trauma, but she had received an intramuscular injection approximately 6 wk earlier. HED scanning showed modest accumulation in the lateral quadriceps muscle. MRI showed high signal intensity in the lateral quadriceps muscle, more suggestive of inflammation than neoplasm. Other focal deposits of HED uptake were present within the skeleton that corresponded well with lesions identified on previous MIBG scintigraphy. Chemotherapy was resumed and MIBG scanning and MRI were performed 1 mo later. At this point, the pain was relieved, and most of the MIBG uptake in the skeleton, as well as the abnormal signal on MRI, had resolved. There was no abnormal MIBG uptake within the muscle on images obtained 3 wk prior to and 4 wk following PET and MRI. We believe that HED uptake within the muscle prior to therapy was due to neuroblastoma, and this disease had largely resolved due to chemotherapy. Inflammation from a prior injection, however, and subsequent healing cannot be totally excluded and, thus, the data from this patient are not included in Figures 3 or 4.

DISCUSSION

Hydroxyephedrine is the first available positron-emitting probe of the sympathetic nervous system suitable for administration in humans (*8*). This compound has been used to investigate the sympathetic innervation of the heart and we have previously described its concentration in pheochromocytoma deposits (*10,11*). In the myocardium, and presumably other organs with sympathetic innervation, HED uptake and retention reflect the functional integrity of the sympathetic neurons (*16*). Unlike norepinephrine, HED contains an alpha-methyl group that prevents metabolism by monamine oxidase. Thus, HED may persist in the cytosol without vesicular storage. Since HED content declines rapidly after blockade of catecholamine uptake mechanisms, retention is largely due to reuptake of HED which has diffused from the neuron into the synaptic cleft (*16*).

In this study, we have shown that HED promptly accumulates

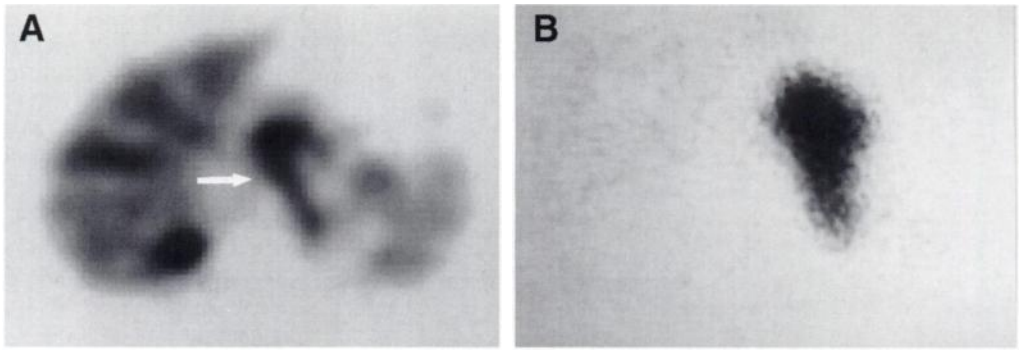

FIGURE 5. Patient 4. (A) HED-PET scan of the midabdomen 30 min postinjection. There is accumulation of HED (arrow) to the left of the liver as well as excretion of HED through the right kidney. (B) MIBG-SPECT scan at 24 hr shows excellent uptake within the neuroblastoma. There is little remaining liver and kidney activity, and thus the tumor appears quite prominent.

in and is well retained by neuroblastomas. Neuroblastomas were demonstrated in all seven patients. Tumors were detected within minutes after tracer injection. Hepatic uptake was prominent quite early but declined progressively. Renal uptake and excretion were likewise prominent early after injection and, like the liver, declined rapidly. Cinematic display of the tomographic data and ROI analysis enable delineation of tumor uptake, which mostly remains stable, from hepatic and renal uptake, which decline. The continuing rise in tumor-to-liver activity through 30 min, principally due to hepatic clearance, suggests that maximal contrast may occur after 30 min. Later images, however, suffer from lower count density due to the rapid decay of the ^{11}C label.

Comparison of MIBG and HED

Patient 1's images and previous studies in patients with pheochromocytoma using [^{123}I]MIBG showed poor tumor visualization until 18–24 hr postinjection. MIBG and HED enter sympathetic neuronal cells through the type 1 catecholamine uptake pump. HED is more polar than MIBG, and there appears to be much less nonspecific uptake early following administration and faster clearance of activity from the liver and kidney. Thus, tumor-to-nontumor accumulation of HED is relatively high early after injection and neuroblastomas are visualized within minutes.

Although MIBG is rapidly removed from the circulation, clearance of background activity proceeds slowly, and this agent requires at least 18–24 hr to achieve tumor-to-nontumor ratios adequate for imaging. As with HED, MIBG retention in neuroblastoma cells is not dependent on vesicular storage. Smets et al. (*17*) showed that imipramine, an inhibitor of catecholamine uptake, causes release of MIBG from neuroblastoma cells, while reserpine, which inhibits transport of catecholamines into storage granules, has little effect. Thus, high intracellular concentrations of MIBG are sustained by re-uptake of MIBG which has diffused from the cells. In pheochromocytoma cells, however, MIBG retention does reflect storage within catecholamine vesicles. As demonstrated by the images of Patient 4, MIBG may be extensively cleared from nontumor tissues by 24 hr, resulting in excellent tumor visualization. In two patients, tumors appeared more striking on [^{123}I]MIBG SPECT images due to greater clearance of MIBG from surrounding tissues at 24 hr than HED clearance at 30 min.

Feasibility of FDG-PET

Fluorine-18-FDG may also be used to evaluate neuroblastoma. The uptake and retention of FDG in tumor tissues reflects the accelerated glycolysis found in many malignancies (*18*). FDG accumulation is independent of type 1 catecholamine uptake. Thus, this agent presents an alternative functional approach for evaluating this tumor (*19*). We are currently studying the utility of this agent for the evaluation of neuroblastoma. In those patients whose tumors were studied with both FDG and HED, uptake of HED was superior, as evidenced by the higher concentration of HED in the tumor of Patient 3 and the lack of tumor visualization in the FDG study of Patient 2. Thus, the pursuit of agents that take advantage of the catecholamine uptake mechanism characteristic of neuroblastoma seems more promising than assessment of a basic metabolic feature.

Potential Advantages of HED-PET

PET with ^{11}C-HED is an approach that utilizes state-of-the-art imaging technology and a newly developed radiotracer probe of sympathetic neuronal activity. There are several potential advantages of this approach compared to conventional scintigraphy with MIBG. These include completion of the study soon after injection of the tracer, improved image resolution of PET over SPECT technology and quantification of tumor uptake. Moreover, the PET approach allows the investigation, using multiple short-lived tracers, of various aspects of tumor biology, such as blood flow, glucose and amino acid metabolism, as well as catecholamine uptake. Our data show that this approach is feasible and possibly useful.

Limitations

The ultimate role for HED–PET imaging in the clinical evaluation of neuroblastoma is uncertain. MIBG is widely available and, when labeled with ^{123}I, produces high quality planar and SPECT images of pheochromocytomas and neuroblastomas. Currently, the costs of HED-PET are high and the availability is limited. The short half-life of ^{11}C requires onsite synthesis for each patient. Our study suggests that a longer-lived radiolabel would be preferable to obtain optimal tumor-to-liver activity ratios with HED. Compounds under development labeled with ^{18}F (half-life 110 min), such as 6-[^{18}F]fluorodopamine, 6-[^{18}F]fluoronorepinephrine, and 6-[^{18}F]fluorometaraminol, may be preferable for delivery to outlying PET centers from regional cyclotron-chemistry units or for studies in several patients and might show superior uptake (*20–22*). Other ^{11}C-labeled probes may also prove to be more highly concentrated in tumor deposits and show less hepatic accumulation (*23–26*). Excretion of HED into the lower urinary tract may impair visualization of tumors in the bladder region, thus necessitating bladder catheterization for optimal evaluation of the pelvis. In addition, PET is not yet ideally suited for whole-body screening (*27*). With the method of Dahlbom (*28*), however, high quality nonattenuation corrected images can be obtained. Larger z-axis field of view PET detectors and three-dimensional image acquisitions may reduce the imaging time considerably, making whole-body studies with ^{11}C tracers more practical.

CONCLUSION

We have shown that high quality functional PET images of neuroblastoma can be obtained promptly after injection of HED. Imaging is limited, however, by the short half-life of the ^{11}C label, and further studies with other positron-emitting agents of the adrenergic nervous system may be useful.

ACKNOWLEDGMENTS

Special thanks to Karen Grahl and Patti Rose for preparation of the manuscript; to Shirley Zempel, RN and Sharon Stetz, RN for patient care assistance; to Diane Lahti, CNMT, Greg Fisher, CNMT, Nancy Tsai, CNMT, Todd Hauser, CNMT, Paul Kison, CNMT, Edward McKenna, CNMT, Jill Rothley, CNMT, and Andrew Weeden, CNMT, for technological expertise and support; to the cyclotron staff for the preparation of ^{11}C; to Markus Schwaiger, MD, Brahm Shapiro, MB, ChB, PhD and David E. Kuhl, MD for stimulating and motivating discussions and to William H. Beierwaltes, MD without whose long-standing interest in neuroendocrine tumors this work would not have been possible.

This work was supported by FIRST Award 1 R29 CA54216 from the National Cancer Institute and grant MO1 RR 00042 from the Clinical Research Center of the University of Michigan.

This work was presented in part at the 1993 European Association of Nuclear Medicine Congress, Lausanne, Switzerland; and at the 40th Annual Meeting of the Society of Nuclear Medicine, 1993, Toronto, Canada.

REFERENCES

1. Finkelstein JZ. Neuroblastoma. The challenge and frustration. *Hematol Oncol Clin N Am* 1987;1:675–694.
2. Kushner BH, Cheung NKV. Neuroblastoma. *Pediatr Ann* 1988;17:269–284.
3. Wieland DM, Wu JL, Brown LE, Mangner TJ, Swanson DP, Beierwaltes WH. Radiolabeled adrenergic neuron blocking agents: Adrenomedullary imaging with ^{131}I-iodobenzylguanidine. *J Nucl Med* 1980;21:349–353.
4. Sisson JC, Frager MS, Valk TW, et al. Scintigraphic localization of pheochromocytoma. *N Engl J Med* 1981;305:12–17.
5. Treuner J, Feine U, Niethammer D, et al. Scintigraphic imaging of neuroblastoma with [^{131}I]iodobenzylguanidine [Letter]. *Lancet* 1984;1:333–334.
6. Shulkin BL, Shapiro B. Radioiodinated meta-iodobenzylguanidine in the management of neuroblastoma. In: Pochedly C, ed. *Neuroblastoma*. Boca Raton: CRC Press; 1990:171–198.
7. Gelfand MJ. Meta-iodobenzylguanidine in children. *Semin Nucl Med* 1993;23:231–242.
8. Rosenspire KC, Haka MS, Jewett DM, et al. Synthesis and preliminary evaluation of [^{11}C]metahydroxyephedrine: a false neurotransmitter agent for heart neuronal imaging. *J Nucl Med* 1990;31:1328–1334.
9. Schwaiger M, Kalff V, Rosenspire KC, et al. The noninvasive evaluation of the sympathetic nervous system in the human heart by PET. *Circulation* 1990;82:457–464.
10. Schwaiger M, Hutchins GD, Kalff V, et al. Evidence for regional catecholamine uptake and storage sites in the transplanted human heart by positron emission tomography. *J Clin Invest* 1991;87:1681–1690.
11. Shulkin BL, Wieland DM, Schwaiger M, et al. PET scanning with hydroxyephedrine: an approach to the localization of pheochromocytoma. *J Nucl Med* 1992;33:1125–1131.
12. Shulkin BL, Wieland DM, Baro ME, et al. PET studies of neuroblastoma with carbon-11-hydroxyephedrine. *J Nucl Med* 1993;33:220.
13. Shulkin BL, Wieland DM, Baro ME, et al. PET studies of neuroblastoma with carbon-11-hydroxyephedrine. *Eur J Nucl Med* 1993;20:858.
14. Khafagi FA, Shapiro B, Fig LM, Mallette S, Sisson JC. Labetalol reduces iodine-131-MIBG uptake by pheochromocytoma and normal tissues. *J Nucl Med* 1989;30:481–489.
15. Paltiel HJ, Gelfand MJ, Elgazzar AH, et al. Neural crest tumors: I-123-MIBG imaging in children. *Radiology* 1994;190:117–121.
16. DeGrado TR, Hutchins GD, Toorongian SA, Wieland DM, Schwaiger M. Myocardial kinetics of carbon-11-meta-hydroxyephedrine: retention mechanisms and effects of norepinephrine. *J Nucl Med* 1993;34:1287–1293.
17. Smets LA, Janssen M, Metwally E, Loesberg C. Extragranular storage of the neuron blocking agent meta-iodobenzylguanidine (MIBG) in human neuroblastoma cells. *Biochem Pharmacol* 1990;39:1959–1964.
18. Hawkins RA, Hoh C, Dahlbom M, et al. PET cancer evaluations with FDG. *J Nucl Med* 1991;32:1555–1558.
19. Shulkin BL, Dole MG, Mitchell DS, Prakash D, Koeppe RA, Hutchinson RJ. PET-FDG studies of neuroblastoma. *Radiology* 1993;189:200p.
20. Eisenhofer G, Hovevey-Sion D, Kopin IJ, et al. Neuronal uptake and metabolism of 2- and 6- fluorodopamine: false neurotransmitters for positron emission tomographic imaging of sympathetically innervated tissues. *J Pharmacol Exp Ther* 1989;225:419–427.
21. Ding YS, Fowler JS, Dewey SL, et al. Comparison of high specific activity (−) and (+)-6-[^{18}F]fluoronorepinephrine and 6-[^{18}F]fluorodopamine in baboons: heart uptake, metabolism and the effect of desipramine. *J Nucl Med* 1993;34:619–629.
22. Schwaiger M, Guiborg H, Rosenspire K, et al. Effect of regional myocardial ischemia on sympathetic nervous system as assessed by fluorine-18-metaraminol. *J Nucl Med* 1990;31:1352–1357.
23. Haka MS, Jung YW, Rosenspire KC, Wieland DM. Synthesis of [^{11}C]-*para*-hydroxyephedrine (PHED)—comparison with the heart agent MHED [Abstract]. *J Nucl Med* 1990;31(suppl):738.
24. Hutchins GD, Van Dort ME, Toorongian SA, Wieland DM. Evaluation of the kinetic properties of [^{11}C] *threo-meta*-hydroxyephedrine (1S, 2S) in dog myocardium. *J Nucl Med* 1991;32:928.
25. Chakraborty PK, Gildersleeve DL, Jewett DM, et al. High yield synthesis of high specific activity R-(−)[^{11}C]epinephrine for routine PET studies in humans. *Nucl Med Biol* 1993;20:939–944.
26. Farde L, Halldin C, Nagren K, Suhara T, Karlsson P, Schoeps K-O. Positron emission tomography shows high specific uptake of racemic carbon-11 labeled norepinephrine in the primate heart. *Eur J Nucl Med* 1994;21:345–347.
27. Hawkins RA, Hoh C, Glaspy J, et al. The role of positron emission tomography in oncology and other whole-body applications. *Semin Nucl Med* 1992;22:268–284.
28. Dahlbom M, Hoffman EJ, Hoh CK, et al. Whole-body positron emission tomography: part I. Methods and performance characteristics. *J Nucl Med* 1992;33:1191–1199.